

Relationship between the shear viscosity and heating rate of metallic glasses below T_g

K. Csach

Institute of Experimental Physics, Slovak Academy of Sciences, Watsonova 47, Košice, Slovakia

O. P. Bobrov, V. A. Khonik,* and S. A. Lyakhov

Department of General Physics, State Pedagogical University, Lenin St 86, 394043 Voronezh, Russia

K. Kitagawa

Graduate School of Natural Science and Technology, University of Kanazawa, Kakuma-machi, Kanazawa 920-1192, Japan

(Received 8 October 2005; revised manuscript received 25 January 2006; published 28 March 2006)

It has been shown that the shear viscosity of bulk and ribbon glassy $\text{Pd}_{40}\text{Cu}_{30}\text{Ni}_{10}\text{P}_{20}$ at temperatures $T < T_g$ (T_g is the glass transition temperature) follows a simple relationship, $\ln \eta(T) = B(T) - \ln \dot{T}$, where \dot{T} is the heating rate and B depends only on temperature. This means, in particular, that $\ln \eta(T)$ dependencies measured at different heating rates can be superposed by a simple vertical shift and the derivative $\partial \ln \eta / \partial \ln \dot{T}|_{T=\text{const}} = -1$. Such a behavior is indeed found for glassy $\text{Pd}_{40}\text{Cu}_{30}\text{Ni}_{10}\text{P}_{20}$. The experimental viscosity data derived earlier on other metallic glasses follow the same relationship. It is argued that this relationship originates from stress-oriented irreversible structural relaxation with distributed activation energies.

DOI: [10.1103/PhysRevB.73.092107](https://doi.org/10.1103/PhysRevB.73.092107)

PACS number(s): 62.20.Hg, 81.05.Kf

I. INTRODUCTION

Metallic glasses (MGs) attract considerable attention due to their unique physical properties and recently developed techniques of preparation of samples in the bulk form.^{1,2} Among the other physical characteristics of MGs, the shear viscosity η is one of the most important kinetic parameters controlling their atomic mobility and, hence, the glass-forming ability and relaxation kinetics of many physical properties below the glass transition temperature T_g .³⁻⁵ In particular, it has been long known that the shear viscosity of MGs changes by orders of magnitude upon structural relaxation below T_g .⁶ It is, therefore, of major importance from both scientific and application viewpoints to study the kinetic viscosity laws upon different experimental conditions.

At a constant temperature, the shear viscosity linearly increases with time (after a short transient), while the viscosity growth rate decreases with temperature, as it was found as far back as in the early eighties.^{7,8} Upon heating at a constant rate \dot{T} , the heating rate dependence of the shear viscosity was first explicitly reported in Ref. 9 for a Co-based ribbon glass. Later, this dependence was reported in Refs. 10–12 for ribbon Finemet $\text{Fe}_{73.5}\text{Cu}_1\text{Nb}_3\text{Si}_{13.5}\text{B}_9$ and ribbon/bulk $\text{Zr}_{52.5}\text{Ti}_5\text{Cu}_{17.9}\text{Ni}_{14.6}\text{Al}_{10}$. It was found that $\eta(\dot{T})$ dependence below T_g is pretty strong and its isothermal cuts show that the viscosity linearly increases with the inverse heating rate. All the aforementioned features of both isothermal and linear heating viscosity behavior below T_g were consistently explained within the framework of the directional structural relaxation (DSR) model^{5,13} as a result of stress-oriented irreversible structural relaxation with distributed activation energies.

In this report, we extend the $\eta(T, \dot{T})$ study on bulk and ribbon $\text{Pd}_{40}\text{Cu}_{30}\text{Ni}_{10}\text{P}_{20}$, which is currently considered as a model nondecomposing (above T_g) glass with exceptionally high glass forming ability and propose a new simple relation-

ship between the shear viscosity and heating rate based on the DSR model.

II. EXPERIMENT

The initial $\text{Pd}_{40}\text{Cu}_{30}\text{Ni}_{10}\text{P}_{20}$ (at. %) master alloy was prepared by direct melting of the components (purity not worse than 99.95) by a two-zone method in a thick-walled quartz vial under controlled phosphorus pressure. A part of this alloy was used to prepare the ribbon (27–34 μm thick and 0.6–0.8 mm wide) by a conventional single roller melt quenching technique. The other part was jet quenched into a copper mold with a $2 \times 5 \times 60 \text{ mm}^3$ cavity. The melt quenching rate R in this case was directly measured by digitizing the signal of a thermocouple placed in the center of the cavity and found to be $70 < R < 350 \text{ K/s}$ near T_g . X-ray microanalysis of bulk bars as well as that of the ribbons showed that the variations of the chemical composition do not exceed 1 at. %. Bulk and ribbon samples were carefully checked by x rays (diffractometer Seifert XRD 300 PTS) to be completely amorphous. Differential scanning calorimetry (DSC) was carried out by a Perkin-Elmer DSC-7 instrument.

The shear viscosity was calculated from linear heating creep data. Tensile creep measurements were performed by a quartz Setaram TMA-92 thermomechanical analyzer and by a homemade quartz instrument with similar characteristics in the range of the heating rates $0.3 \leq \dot{T} \leq 10 \text{ K/min}$. The gauge length of samples was about 15 mm while the sensor resolution was set in-between 0.1 and 0.01 μm depending on the heating rate. At a given heating rate and sample type (bulk/ribbon), the creep test was taken twice, under the tensile stresses of about 8 and 120 MPa (held to within 10%–15%). The runs under 8 MPa were used as reference measurements and, to eliminate the unwanted thermal expansion of the instruments, were subtracted from the creep data taken at

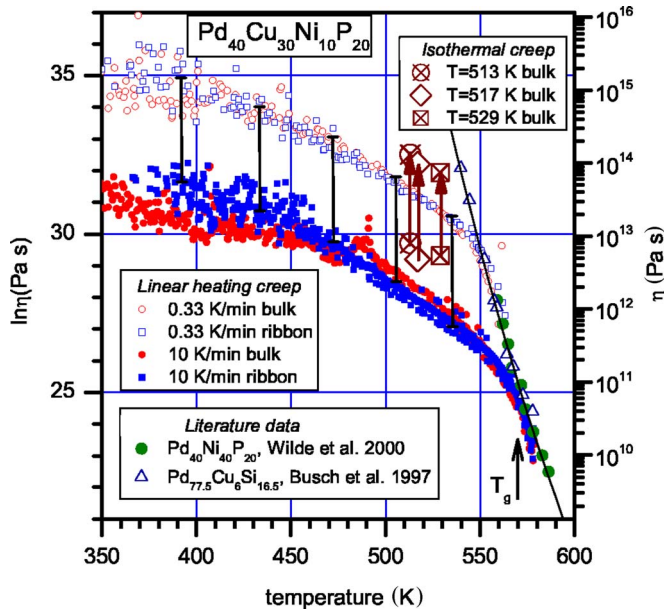


FIG. 1. (Color online) Temperature dependencies of the logarithm of the shear viscosity of bulk and ribbon $\text{Pd}_{40}\text{Cu}_{30}\text{Ni}_{10}\text{P}_{20}$ at two indicated heating rates. Literature data on the equilibrium shear viscosity of similar glasses are also shown. The arrow denotes the glass transition temperature measured by DSC at 5 K/min. It is seen that the $\ln \eta(T)$ dependencies below T_g are nearly parallel each other as shown by five equal vertical bars, in accordance with the expectations, see the text. Isothermal viscosity changes of bulk samples at $T=513$, 517, and 529 K are given for a comparison.

120 MPa (see Ref. 9 for details). Every differential tensile strain-temperature curve was subjected to a ten-point adjacent averaging and numerically differentiated after that. The shear viscosity was then calculated as $\eta = \sigma_{eff} / 3\dot{\epsilon}_{eff}$, where the effective plastic strain rate $\dot{\epsilon}_{eff} = \frac{d}{dt}(\epsilon - \epsilon_{ref})$, ϵ is the strain determined under the stress σ (≈ 120 MPa), ϵ_{ref} is the strain measured under the stress σ_{ref} (≈ 8 MPa), and the effective stress $\sigma_{eff} = \sigma - \sigma_{ref}$.

III. RESULTS AND DISCUSSION

Figure 1 shows temperature dependencies of the logarithm of the shear viscosity of bulk and ribbon $\text{Pd}_{40}\text{Cu}_{30}\text{Ni}_{10}\text{P}_{20}$ at the heating rates of 0.33 and 10 K/min. The literature data by Busch *et al.*¹⁴ and Wilde *et al.*¹⁵ on the quasiequilibrium viscosity (i.e., in the supercooled liquid state) of similar glasses (approximated by a straight line) are also shown. The arrow gives the glass transition temperature determined as a midpoint between the two tangents drawn below and above the glass transition region on a DSC curve taken at 5 K/min. The following features are to be noted.

(i) There is a strong heating rate dependence of the shear viscosity below T_g similar to other MGs (Refs. 10–12) while at $T \geq T_g$ the $\ln \eta(T, \dot{T})$ curves merge defining a clear quasiequilibrium viscosity curve together with the aforementioned literature data.

(ii) The merge of the viscosity data above T_g is in sharp contrast with previous investigations^{11,12} of bulk and

ribbon $\text{Zr}_{52.5}\text{Ti}_5\text{Cu}_{17.9}\text{Ni}_{14.6}\text{Al}_{10}$, which showed a strong $\eta(\dot{T})$ dependence even above T_g (although in that case η increased with \dot{T} , contrary to the $T < T_g$ temperature range). It was discussed earlier that this feature of Zr glass could be explained by its phase decomposition above T_g .^{11,12}

(iii) Within the data scatter, we did not find any notable differences in the viscosity behavior of bulk and ribbon samples both below and above T_g , in spite of a distinction of about four orders of magnitude in the production quenching rates. This rather surprising finding will be discussed in a separate publication. It could be just briefly mentioned that a minor effect of such a huge change of the production quenching rate was earlier noticed upon measurements of linear heating internal friction¹⁶ and isothermal stress relaxation¹⁷ of bulk/ribbon glassy $\text{Zr}_{52.5}\text{Ti}_5\text{Cu}_{17.9}\text{Ni}_{14.6}\text{Al}_{10}$, creep¹² and isothermal/linear heating stress relaxation¹⁸ of bulk/ribbon $\text{Pd}_{40}\text{Cu}_{30}\text{Ni}_{10}\text{P}_{20}$. It turns out, therefore, that such a behavior could be characteristic of MGs. According to generally accepted classical phenomenological picture of the glass transition as a kinetic phenomenon,¹⁹ a change of the production quenching rate must result in a change of the density while the latter determines the amount of the free volume. The independence of aforementioned viscoelastic and anelastic properties on the production quenching rate, therefore, could question the role of the free volume as a key parameter controlling the kinetics of structural relaxation and related viscoelastic phenomena.^{17,18}

(iv) Five equal vertical bars in Fig. 1 show that the $\ln \eta(T)$ dependencies taken at different heating rates can be superposed just by a parallel shift along the ordinate axis. This procedure is valid for all temperatures, which are lower than T_g by 20–30 K. It should be emphasized that the same situation could be noticed for Finemet $\text{Fe}_{73.5}\text{Cu}_1\text{Nb}_3\text{Si}_{13.5}\text{B}_9$ (Ref. 10) (this glass does not display any caloric glass transition and the viscosity curves can be superposed by a vertical shift just almost exactly) and bulk/ribbon $\text{Zr}_{52.5}\text{Ti}_5\text{Cu}_{17.9}\text{Ni}_{14.6}\text{Al}_{10}$ (see Fig. 2 in Ref. 12). Since this superposition seems to be a common feature of MGs, it is worth close attention. This feature could be understood as follows.

Irreversible structural relaxation occurring below T_g has a pronounced effect on the viscous flow behavior of MGs. For instance, three arrows in Fig. 1 show the *isothermal* viscosity growth of three different as-cast bulk samples heated up to $T=513$, 517, and 529 K at a rate of 5 K/min, preannealed for ≈ 100 s and tested under stress at these temperatures for 14 000 s. It is seen that this relatively short annealing increases the shear viscosity by about an order of magnitude. Meanwhile, it was reported long ago that the shear viscosity of MGs at a given temperature can increase by five orders of magnitude as a result of irreversible structural relaxation.⁶ The effect of irreversible structural relaxation on various viscoelastic properties (isothermal and linear heating creep, stress relaxation, low frequency internal friction, and strain recovery) was recently successfully described within the framework of the aforementioned DSR model (see Refs. 5, 13, and 20 for a review of the model and its application to structural relaxation-induced viscoelastic phenomena). For the shear viscosity upon linear heating at a rate \dot{T} , the DSR model gives^{5,13}

$$\eta(T) = \{N_0[E_0(T)]\Omega CA\dot{T}\}^{-1}, \quad (1)$$

where N_0 is the volume density of “relaxation centers” per unit activation energy interval, C is a parameter accounting for the orienting effect of the external stress on irreversible rearrangements in relaxation centers, which on the average comprise a volume Ω , and E_0 is the characteristic activation energy of these rearrangements connected with current temperature according to $E_0 = AT$ with $A \approx 3.1 \times 10^{-3}$ eV/K. Equation (1) can be rewritten as

$$\ln \eta(T) = B(T) - \ln \dot{T}, \quad (2)$$

where $B = -\ln(N_0\Omega CA)$ depends only on temperature (activation energy). Equation (2) shows that if viscosity measurements are done under two different heating rates, \dot{T}_1 and \dot{T}_2 , then the relationship

$$\ln \frac{\eta_1(\dot{T}_1)}{\eta_2(\dot{T}_2)} = \ln \frac{\dot{T}_2}{\dot{T}_1} \quad (3)$$

should be valid for any temperature. For instance, if like in Fig. 1, $\dot{T}_1 = 10$ K/min and $\dot{T}_2 = 0.33$ K/min, then the logarithm of the ratio of the corresponding viscosities should be equal to $\ln(10/0.33) \approx 3.41$ at any temperature $T < T_g$. Therefore, on the $\ln \eta(T)$ plot, the two viscosity curves taken at aforementioned heating rates should be separated by the amount of 3.41 along the ordinate axis. Returning back to Fig. 1, one can notice that the viscosity curves are shifted by the length of a vertical bar, which equals to ≈ 3.3 , in excellent agreement with the prediction of Eq. (2).

On the other hand, Eq. (2) implies that for any temperature $T = \text{const}$, $\ln \eta$ should linearly decrease with $\ln \dot{T}$ and the angle coefficient of this dependence should be $k = \partial \ln \eta / \partial \ln \dot{T}|_{T=\text{const}} = -1$. This prediction could be checked by making isothermal cuts of temperature dependencies of the shear viscosity measured at different heating rates. The corresponding results for bulk and ribbon $\text{Pd}_{40}\text{Cu}_{30}\text{Ni}_{10}\text{P}_{20}$ are given in Fig. 2 for the cuts taken at $T = 400, 425, 450, 500,$ and 525 K. The root-mean-square linear approximations of $\ln \eta(\ln \dot{T})$ data and the corresponding angle coefficients k together with their standard deviations are also shown. It is seen that the angle coefficients within the data scatter are indeed close to -1 . It is also worthy of notice that we did not find any statistically significant difference between the data taken on bulk and ribbon samples.

Another way to check Eq. (1) is to plot η as a function of the inverse heating rate at $T = \text{const}$. It was carefully shown earlier^{5,11,12} on ribbon Finemet $\text{Fe}_{73.5}\text{Cu}_1\text{Nb}_3\text{Si}_{13.5}\text{B}_9$ and ribbon/bulk $\text{Zr}_{52.5}\text{Ti}_5\text{Cu}_{17.9}\text{Ni}_{14.6}\text{Al}_{10}$ that such a dependence is indeed observed.

It is to be concluded, therefore, that Eq. (1) and its modifications [Eqs. (2) and (3)] provide a good explanation for the shear viscosity behavior upon linear heating with different heating rates below T_g . Since this equation was derived within the DSR model and taking into account the fact that this model gives a good description of other structural relaxation-induced viscoelastic properties of MGs, one can

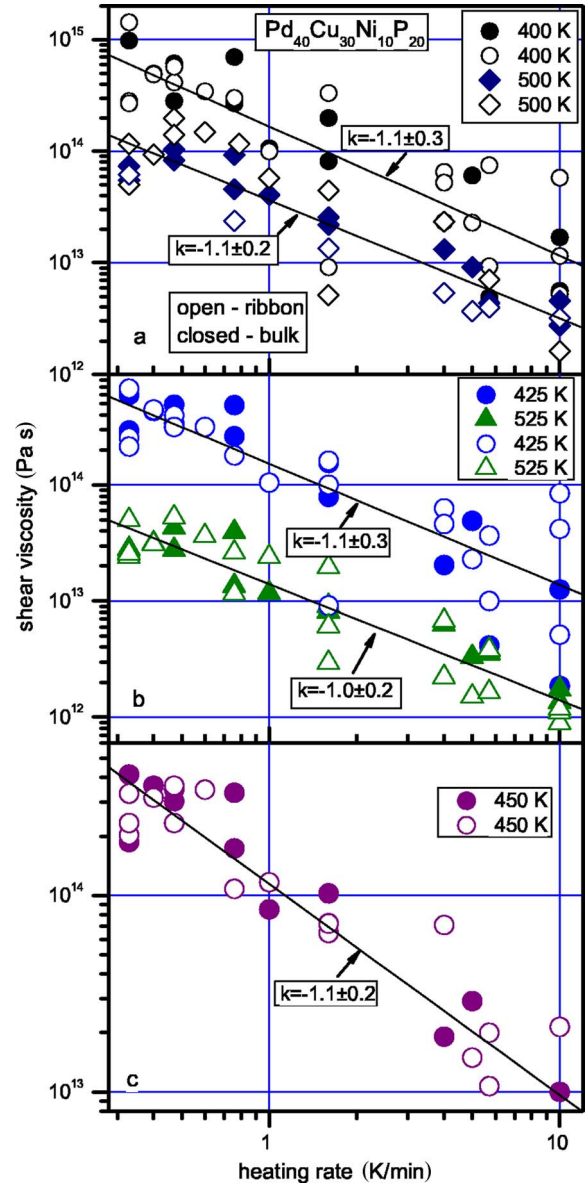


FIG. 2. (Color online) The shear viscosity of bulk (closed symbols) and ribbon (open symbols) $\text{Pd}_{40}\text{Cu}_{30}\text{Ni}_{10}\text{P}_{20}$ at indicated temperatures as a function of the heating rate on the logarithmic scales on both axes. It is seen that $\ln \eta(\ln \dot{T})$ dependencies within the error can be approximated by a straight line with the angle coefficient $k = \partial \ln \eta / \partial \ln \dot{T} = -1$, in accordance with Eq. (2).

assert that the shear viscosity behavior of metallic glasses upon linear heating below T_g is conditioned by irreversible structural relaxation, as implied by the DSR model. Within the framework of the latter, irreversible structural relaxation is viewed as a set of stress-oriented local irreversible two-stage atomic rearrangements with continuously distributed activation energies.^{5,13,20}

IV. CONCLUSIONS

Detailed linear heating creep study of bulk and ribbon glassy $\text{Pd}_{40}\text{Cu}_{30}\text{Ni}_{10}\text{P}_{20}$ has been performed. No significant

difference between the shear viscosity behavior of bulk and ribbon samples has been found, in spite of a four-orders-of-magnitude difference in the production quenching rates.

Below T_g , the temperature dependencies of the shear viscosity measured at different heating rates follow a simple relationship given by Eq. (2), which was derived within the framework of the DSR model. Consequently, two viscosity curves measured at two heating rates, \dot{T}_1 and \dot{T}_2 , can be superposed by a shift equal to $\ln(\dot{T}_2/\dot{T}_1)$ along the $\ln \eta$

axis, as exemplified by Fig. 1. At $T=\text{const}$, the logarithm of the shear viscosity linearly decreases with logarithm of the heating rate and the corresponding angle coefficient within the error equals to minus one, in accordance with Eq. (2). The fact of applicability of Eq. (2) strongly implies that the heating rate dependence of the shear viscosity of metallic glasses originates from stress-oriented irreversible structural relaxation with continuously distributed activation energies.

*Electronic address: khonik@vspu.ac.ru

¹W. L. Johnson, MRS Bull. **24**, 42 (1999).

²A. Inoue, *Bulk Amorphous Alloys. Practical Characteristics and Applications. Materials Science Foundation* (Transtech, Zurich, 1999), Vol. 6.

³R. Busch, Ann. Chim. (Paris) **27**, 3 (2002).

⁴S. Mukherjee, J. Schroers, W. L. Johnson, and W.-K. Rhim, Phys. Rev. Lett. **94**, 245501 (2005).

⁵V. A. Khonik, J. Non-Cryst. Solids **296**, 147 (2001).

⁶A. I. Taub and F. Spaepen, Scr. Metall. **13**, 195 (1979).

⁷A. I. Taub and F. Spaepen, Acta Metall. **28**, 1781 (1980).

⁸A. I. Taub and F. E. Luborsky, Acta Metall. **29**, 1939 (1981).

⁹V. A. Khonik, V. A. Mikhailov, and I. A. Safonov, Scr. Mater. **37**, 921 (1997).

¹⁰V. A. Khonik, M. Ohta, and K. Kitagawa, Scr. Mater. **45**, 1393 (2001).

¹¹A. E. Berlev, O. P. Bobrov, K. Csach, V. L. Kaverin, V. A. Khonik, K. Kitagawa, J. Miškuf, and A. Juríková, J. Appl. Phys. **92**, 5898 (2002).

¹²A. E. Berlev, O. P. Bobrov, V. A. Khonik, K. Csach, A. Juríková, J. Miškuf, H. Neuhäuser, and M. Yu. Yazvitsky, Phys. Rev. B **68**, 132203 (2003).

¹³V. A. Khonik, Phys. Status Solidi A **177**, 173 (2000).

¹⁴R. Busch, A. Masuhr, E. Bakke, and W. L. Johnson, Mater. Res. Soc. Symp. Proc. **455**, 369 (1997).

¹⁵G. Wilde, G. P. Görlner, R. Willnecker, and H. J. Fecht, J. Appl. Phys. **87**, 1141 (2000).

¹⁶O. P. Bobrov, V. A. Khonik, S. N. Laptev, and M. Yu. Yazvitsky, Scr. Mater. **49**, 255 (2003).

¹⁷O. P. Bobrov, V. A. Khonik, K. Kitagawa, and S. N. Laptev, J. Non-Cryst. Solids **342**, 152 (2004).

¹⁸O. P. Bobrov, K. Csach, V. A. Khonik, K. Kitagawa, S. N. Laptev, and M. Yu. Yazvitsky, Scr. Mater. **54**, 369 (2006).

¹⁹P. G. Debenedetti and F. H. Stillinger, Nature (London) **410**, 259 (2001).

²⁰V. A. Khonik, Solid State Phenom. **89**, 67 (2003).